Chimia 53 (1999) 67–71

ISSN 0009–4293

OWLS: A Versatile Technique for Sensing with Bioarrays

Jeremy J. Ramsden*

Abstract. Optical waveguide lightmode spectroscopy (OWLS) is introduced as a precision technique capable of yielding detailed information on the structure of biological thin films, and on the kinetics of binding events between biopolymers. Unlike previous methods, it can be applied *in situ* under conditions closely approximating those of a living organism, without the need to label any of the molecules.

1. Introduction – the Genesis of OWLS at the Biozentrum

About a decade ago, the Department of Biophysical Chemistry started to investigate the effects of oligopeptides on lipid-bilayer membranes. Many of these peptides, as well as other small molecules such as polyene antibiotics, enhance the electrical conductivity of the membrane, although individually they are too small to create an ion channel through the bilayer. A still largely unresolved question is, whether they oligomerize to form larger structures, or whether they globally alter the membrane structure, changing its ion permeability. A piece of information essential for resolving this issue is the number r of peptide molecules actually incorporated into the membrane. This quantity cannot be determined directly from classical electrical measurements, but has been estimated from the incorporation of peptides into lipid vesicles (see, *e.g.*, [1]).

In order to simultaneously measure r and its effect (on transmembrane conductivity), work was initiated on the impedance spectroscopy of membranes supported on a planar semiconductor electrode, using the *Langmuir-Blodgett* technique to deposit the lipids [2]. The idea was to determine r from changes in the semiconductor space charge, and hence the imaginary part of the complex impedance, due to the presence of α-helical, and thus dipolar, membrane-spanning peptides. Simultaneously, the membrane conductivity could be obtained from the real part of the impedance. Despite the advantage of increased membrane lifetime (the fragility of a freely suspended lipid-bilayer membrane is a disadvantage of the classical electrical method) by two orders of magnitude – membranes could be used for tens of hours rather than tens of minutes – and the suitability of smooth hydrated silica as a bilayer substrate, the complicated intrinsic impedance of the $Si–SiO_2–H_2O_{(surface)}$ structure prevented satisfactory results from being obtained with this scheme.

At that time, optical methods for probing membrane structure were coming into prominence. Early attempts to determine the refractive index of a lipid-bilayer membrane directly from its reflectance had produced rather contradictory results [3], and neither ellipsometry, nor scanning angle reflectometry (SAR) which was being developed in Strasbourg as a method for investigating adsorbed molecular layers, seem to have been considered to be sufficiently sensitive to be capable of yielding useful data on supported lipid bilayers. But the invention (at the ETH in Zürich) of a method for producing extremely-high quality, yet low-cost, precision gratings in planar optical waveguides opened up a further possibility: measurement of the phase velocities of guided lightmodes in the waveguide in order to characterize the structure of a membrane coating the waveguide. Since many modes can be measured, much more information than a single refractive index is potentially available. The possibility of using integrated optics – *i.e.*, light propagating in waveguides – to investigate surface phenomena had been noted soon after its inception [4]. The method was applied to the characterization of polymer layers [5], but the experimental arrangement was cumbersome and costly, and no further work seems to have appeared until our first publication on the topic [6].

The dramatic cost reduction of the necessary precision gratings awakened our interest in the possibilities of integrated optical measurements to investigate membrane structure in detail. Supported lipid bilayers had already been established as an attractive system at the Biozentrum. Apart from their stability, it could be presumed that a water layer between the (hydrated) support and the bilayer, comparable to the interbilayer water in multilayer stacks (*i.e.*, *ca.* 2.4 nm thick [7]), ensured that the membrane was endowed with a fluidity comparable to that of a cell membrane [8], in contrast to lipid monolayers deposited on alkane-coated substrates, which are frozen in the rigid gel-phase, and hence are not good surrogates for natural membranes. A further advantage of the supported-membrane configuration is the fact that it is very easy to design a flow-cell arrangement such that solutions of small molecules at defined concentrations can be brought into contact with the membrane at will.

An optical waveguide has to have a higher refractive index than its surroundings, and a convenient structure is a thin (*ca.* 200 nm) high-refractive-index layer (*e.g.*, TiO_2) supported on glass. We use

*Correspondence: Dr. J.J. Ramsden
Department of Biophysical Chemistry
Biozentrum
CH-4056 Basel
Tel.: +41 61 267 21 93
Fax: +41 61 267 21 89
E-Mail: ramsden@ubaclu.unibas.ch

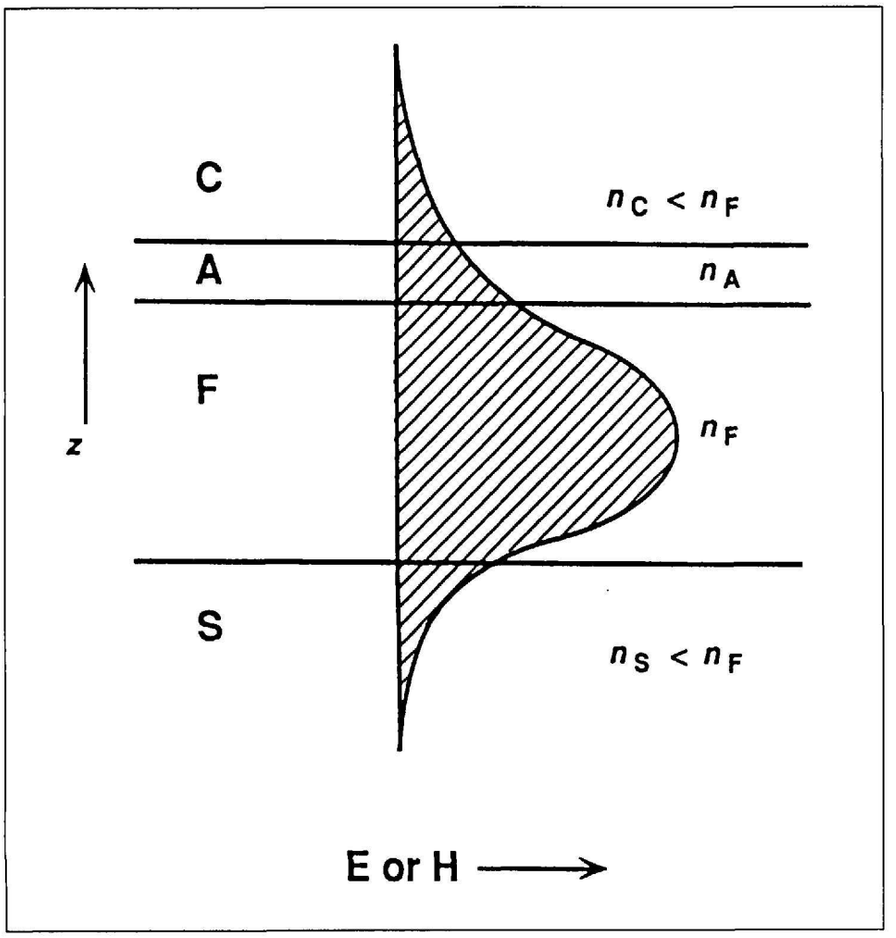

Fig. 1. *Schematic representation of an optical waveguide showing the high-refractive-index layer F, the optical glass support S, the membrane or molecular adlayer A, and the cover medium C.* The shaded area indicates the electromagnetic field distribution of the zeroth-order mode, and the refractive indices are denoted by *n*.

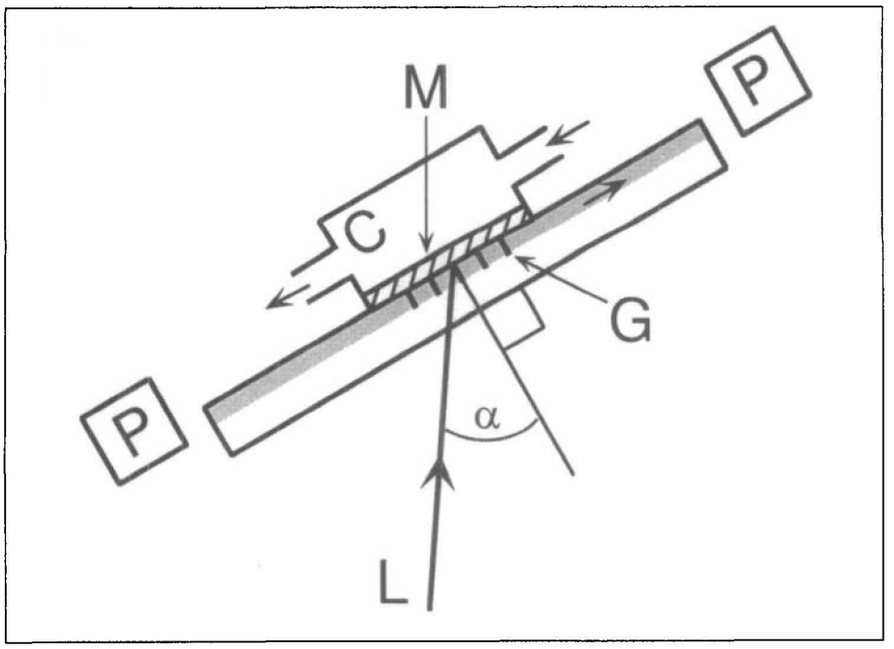

Fig. 2. *Schematic representation of a possible OWLS setup.* L: external light beam incident with angle α onto grating G; P: photodiodes; C: cuvette through which liquid is flowing. M denotes a membrane deposited onto the waveguide. This particular arrangement is used in the *IOS-1* instrument manufactured by *Artificial Sensing Instruments*, Zürich. The light source is a linearly polarized He-Ne laser (wavelength λ = 632.8 nm).

pyrolyzed sol-gel waveguides incorporating a shallow embossed grating. The high-temperature pyrolysis which concludes their manufacture ensures that the waveguide surface is extremely smooth and free of organic contamination.

Fig. 1 shows an optical waveguide, together with the electromagnetic field distribution of the zeroth order (enodal) mode. The characteristic decay length of the evanescent portion can be easily controlled by varying the waveguide parameters [4]. Interaction between the evanescent field and molecules in the interfacial region determines the phase velocities v of the guided waves. *Fig. 2* shows how a grating can be used to measure v. Low-order guided modes are discrete and characterized by an effective refractive index N ($=c/v$). Denoting the wave vector $2\pi/l$ of light *in vacuo* by k, then the guided mode has a wave vector kN. The component of an external light beam in the direction of propagation of the guided wave is $kn \cdot \sin\alpha + 2\pi l/\Lambda$ after diffraction, where α is the angle with which the beam is incident onto the grating, l the diffraction order, and Λ the grating constant. A guided wave is excited when these two are matched, *i.e.*,

$$kN = kn \cdot \sin\alpha + 2\pi l/\Lambda \qquad (1)$$

where n is the refractive index of the external medium (usually air). Hence, N can be determined by monitoring the angles at which guided modes appear. In the arrangement illustrated in *Fig. 2*, this is done by means of photodiodes situated at the ends of the waveguide. The result is a spectrum of modes – thus the name optical waveguide lightmode spectroscopy (OWLS). Currently, N can be determined to a precision of *ca.* 1 ppm [9]. Other measurement configurations are also possible [10].

2. Membrane Structure

Details of the molecular structure of lipid-bilayer membranes can be inferred from the membrane birefringence [8]. One of the great advantages of OWLS is that measurements can be carried out *in situ* while changing the membrane environment. OWLS can be the basis for a (bio)-chemical sensor for drugs [11], or help to elucidate the nature of nonelectrical effects of oligopeptides on membranes (*Fig. 3*).

Other biological membranes, such as the basement membranes external to cells, assembled from secreted proteins such as

fibronectin and laminin, can also be readily investigated. Since OWLS measurements can be carried out over time scales ranging from milliseconds to tens of hours, the assembly of such structures can be monitored in *situ* in real time [12].

3. Protein-Membrane Interactions

The association and dissociation of proteins to the numerous lipid-bilayer membranes within and enclosing cells are among the most ubiquitous types of interaction in biology. Since both model and natural membranes can be assembled on an optical waveguide, OWLS is eminently suited for monitoring protein-membrane binding. No special labelling of either lipid or protein is required, and apart from the high sensitivity and time resolution of the method, the binding can take place under closely controlled hydrodynamic conditions. This is particularly important if binding energies are to be determined from kinetic data [14].

3.1. *Protein Arrays*

The natural fluidity of a biological membrane endows proteins associated peripherally, or attached *via* an anchor partly penetrating into the membrane interior, with considerable lateral mobility. If the proteins have some lateral affinity for each other, ordered arrays can be built up. Array assembly has a dramatic kinetic signature, most easily seen when the binding rate dv/dt is plotted against the amount v of bound protein (*Fig. 4*). This offers a rapid and unambiguous way to screen possible conditions necessary for assembly.

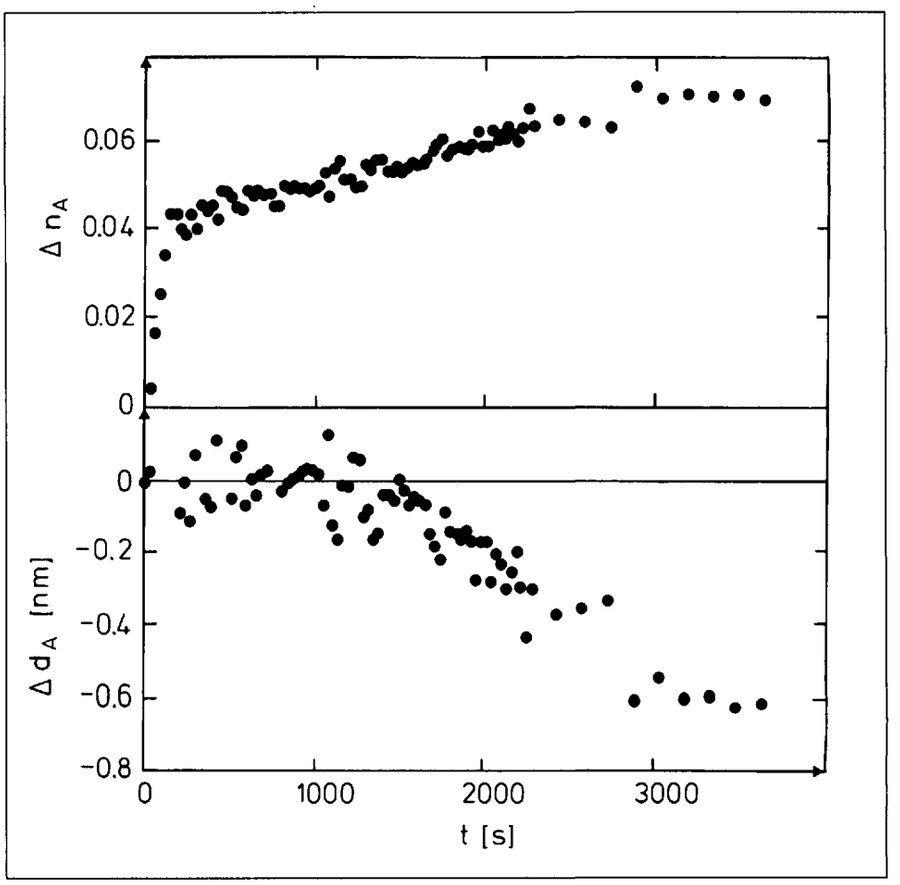

Fig. 3. *The change of mean refractive index and thickness* (Δn_A and Δd_A, respectively) *of a 1-palmitoyl-2-oleoyl-*sn*-glycero-3-phosphatidylcholine bilayer while mellitin, dissolved at a concentration of 1* μM *in 10* μM *2-(*N*-morpholino)ethanesulfonic acid/NaOH, pH 6.0 plus 0.1* M *NaCl, flows over the membrane at a wall-shear rate of 2.7* s^{-1}. The resolution of n_A and d_A are estimated as ± 0.002 and ±1 Å, respectively. Note the apparent occurrence of interdigitation. This has been inferred from X-ray crystallography of lipid-bilayer assemblies [13], but never previously *in situ* for a lipid bilayer. Measurements were carried out with an *IOS-1* integrated optical scanner (*Artificial Sensing Instruments*, Zürich).

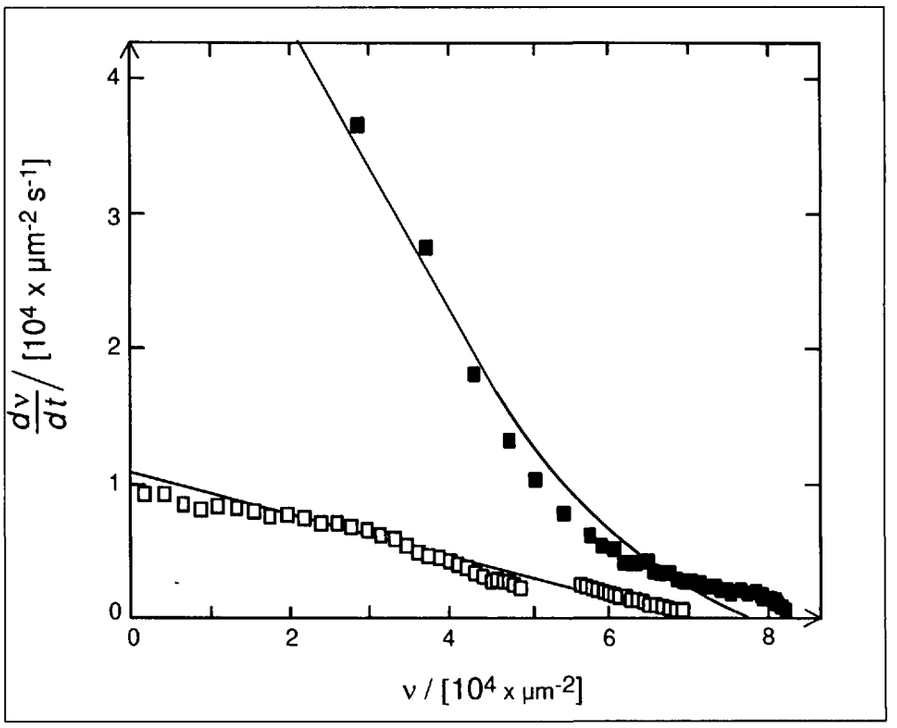

Fig. 4. *The binding of cytochrome P450 1A2* (extracted from the livers of rabbits fed on a diet enriched with 3-methylcholanthrene) *to a bilayer of 1,2-dioleoyl-*sn*-glycero-3-phosphatidylcholine at two different concentrations* [15], *0.3* μM (□) *and 3* μM (■). At the higher bulk concentration, the membrane quickly fills up and the proteins are forced to remain essentially where they first landed. Hence, the rate $dv/dt \propto 1 - 4\theta + (6\sqrt{3}/\pi)\theta^2 + \ldots$ [16] (solid line), where θ is the fraction of total membrane area covered by protein. At the lower concentration, the proteins have time to diffuse laterally and self-assemble into an ordered array with a unit cell 14 nm² in extent, and $dv/dt \propto 1 - \theta$, since the exclusion zones which give rise to the polynomial in θ are annihilated.

3.2. *Biosensors*

It is obvious that OWLS can be used for biosensing in its own right. The typical biosensor configuration calls for a layer of receptors (*e.g.*, proteins) to be immobilized at the surface of a transducer (in this case, the waveguide). Many transducing strategies exist, but there is a problem they all have in common: how can the receptors be immobilized without destroying their biological activity? Usually, covalent linking and crosslinking adversely affect activity. Membrane *anchoring via* an attached hydrophobic moiety maintains a biomimetic environment in which full activity is more likely to be retained [17].

Since OWLS can yield more detailed structural information with fewer assumptions than most other methods currently in use for investigating protein binding to surfaces (adsorption) [18], it is also valuable as a 'sensor of sensors' for studying receptor arrays destined for use in other sensing devices. OWLS represents a good compromise between methods capable of approaching atomic resolution, but which often require highly perturbing sample-preparation procedures and are not available for *in situ* measurements in solution; and other methods appropriate for *in situ* measurements providing particular pieces of information, but which cannot yield very reliable data on the *number* of bound molecules, which is of course an essential parameter for interpreting the others. High-resolution transmission electron microscopy is an example of the former type; an example of the latter is infrared spectroscopy (FTIR), which is potentially able to provide a detailed picture of bonding within the adsorbed layer, but in practice, the spectra are complex and difficult to interpret reliably, and while it is true that the spectrum depends sensitively even on the orientation of the IR-active groups, at present this is a drawback, since it hampers correct assignments. In between these two lies the quartz-crystal microbalance (QCM) [19]. Used in liquids, the observed resonance frequency modulation can potentially yield very interesting data on the viscoelasticity of the adsorbed protein layer (and hence, *inter alia*, its hydration), and on interfacial slip, for which theory has been recently developed [20], although a demonstration of the practical application of this theory is still awaited.

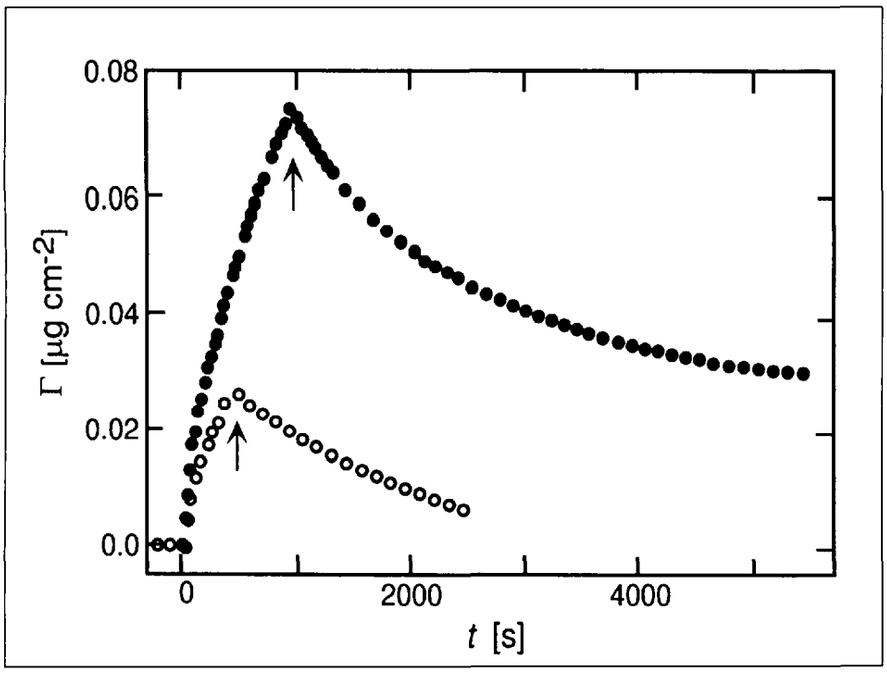

Fig. 5. *Adsorption of the type-IC restriction enzyme* EcoR124/II *from a flowing buffer solution to specific DNA* (●) *and nonspecific (lacking the recognition sequence for the enzyme) DNA* (○) [23]. At the times marked with arrows, the enzyme solution was replaced by pure buffer. The rate coefficients evaluated from the data are, nonspecific association, 30 and 16 M^{-1} s^{-1} for the specific and nonspecific DNA, respectively; nonspecific dissociation, 7.2 and 8.0 × 10^{-4} s^{-1} respectively; and specific association, 2.3 × 10^{-4} and 0 s^{-1}. To achieve the same rate of specific binding solely *via* transport in three dimensions would require the enzyme to bind with a rate exceeding the diffusion limit by at least an order of magnitude, assuming that the cytoplasm has the viscosity of water; in reality, it is much more viscous. The slight difference between the nonspecific coefficients for the two types of DNA may be attributable to slight differences in DNA structure, which may affect binding affinity [24].

4. Biocompatibility

Almost without exception, the first event to occur when an artificial surface is brought into contact with the interior of a living organism is that it becomes covered with a layer of protein. For objects in the bloodstream, the composition of this layer may become exceedingly complex (especially if an immune response is triggered!); if the object is embedded in tissue, cells will adhere to the initial protein deposit. The structure of the initial layer is usually decisive in determining the course of subsequent events. In this regard, OWLS has proved to be very useful; indeed, one of its early successes was the verification that protein adsorption to a continuous surface (*i.e.*, one lacking specific adsorption sites) such as an oxide-coated metal is accurately described as random sequential adsorption (RSA) [21]. RSA gives rise to the characteristic polynomial seen in plots of $d\upsilon/dt$ *vs.* υ (*Fig. 4*). Clearly, this kind of study can be extended to the investigation of microbial colonization of implants under natural conditions.

5. Biological Processes

Since so much biology happens at interfaces, OWLS has great potential for the quantitative characterization of a broad variety of interactions. Most of the traditional methods used to investigate interactions in the molecular-biological laboratory (such as polyacrylamide-gel electrophoresis) suffer from one or more of the following disadvantages: they are slow, expensive, not very accurate, are not very reproducible, need too much material, are difficult to interpret quantitatively. The last point is one that is likely to become increasingly prominent. Since very often 'the devil lies in the details', it will no longer be adequate to merely assign '–' or '+' or even '++' to a binding reaction in order to arrive at a molecular-level understanding (let alone sub-molecular!). We will need to know accurate association constants, stoichiometries, and more. *Dissociation* is often the *Cinderella* of binding studies, yet it seems that the more one looks, the more one finds that dissociation does *not* follow the easily understood and interpreted exponential-decay model, but actually needs a time-dependent rate coefficient to describe it. High-quality dissociation data are needed for characterizing such processes. These are readily available from a typical OWLS experiment (*e.g.*, *Fig. 5*). Firstly, adsorption is allowed to take place (from $t = 0$ to the times marked

with arrows), and then, the adsorbate solution is replaced by pure solvent. The evaluation procedure begins with quantification of the dissociation by fitting that part of the curve at times beyond the arrow to pure dissociation kinetics. Once the dissociation-rate coefficients have been determined, the initial part of the curve is fitted by association-dissociation kinetics, and the association-rate coefficient determined.

In this brief survey, it is clearly impossible to deal with specific cases, which may in fact be found in almost every laboratory at the Biozentrum. As a single example, let us look at the action of restriction enzymes on viral DNA infecting the bacterium *E. coli*. The restriction enzyme is a large, complex molecule, costly to make and maintain, and the bacterium has evolved to synthesize the minimum number necessary, which presumably reflects a trade-off between risk of infection and cost of prevention. Once infection by a phage particle does occur, the bacterium has to act quickly, because the phage DNA is replicated within 15 min. After 45 min, the whole bacterial colony is at risk because the initially infected bacterium lyses, releasing about two hundred new viruses ready to infect the surrounding cells.

The restriction enzyme can recognize a single, short base-sequence on the viral DNA. Looking for this sequence by random diffusion in three dimensions can be compared to the proverbial search for a needle in a haystack, and has a vanishingly small probability of success. Luckily, the recognition sequence is attached to a long piece of 'hay', the entire bacterial DNA molecule. As soon as the enzyme encounters any part of the DNA, it binds nonspecifically, just strongly enough to enable it to execute a random walk along the DNA to search for the recognition sequence; in one dimension rather than three, which is much more efficient [22]. We have measured the association and dissociation of the enzyme to specific DNA sequences at the surface of an optical waveguide, with nonspecific DNA sequences lacking the recognition site as a control (*Fig. 5*). From the numerical values of the rate coefficients, we could deduce that 40–50 enzyme molecules within one bacterium would protect it almost perfectly from attack by one or two phage particles [23].

I should especially like to express my appreciation of the work of my graduate students *Roger Kurrat* and *Gábor Csúcs*, who contributed so much to the early pioneering OWLS measurements. I am, of course, indebted to all my colleagues at the Biozentrum for providing an enduringly stimulating environment for interdisciplinary biophysical chemistry, and to my partners in the *Eureka MEMOCS* project, who have provided indispensable technical help in the continuing improvement of the OWLS technique.

Received: November 12, 1998

[1] V. Rizzo, S. Stankowski, G. Schwarz, *Biochemistry* **1987**, *26*, 2751.
[2] a) J.J. Ramsden, *Ferroelectrics* **1989**, *94*, 473; b) J.J. Ramsden, *Stud. Biophys.* **1989**, *130*, 83.
[3] a) C. Huang, T.E. Thompson *J. Mol. Biol.* **1965**, *13*, 183; b) R.J. Cherry, D. Chapman *ibid.* **1967**, *30*, 551; c) R.J. Cherry, D. Chapman *ibid.* **1969**, *40*, 19.
[4] P.K. Tien, *Appl. Optics* **1971**, *10*, 2395.
[5] J.D. Swalen, M. Tacke, R. Santo, J. Fischer, *Optics Comm.* **1976**, *18*, 387.
[6] J.J. Ramsden, *J. Phys. Chem.* **1993**, *97*, 4479.
[7] J.R. Scherer, *Proc. Natl Acad. Sci. USA* **1987**, *84*, 7938.
[8] J.J. Ramsden, *Phil. Mag. B* **1999**, *79*, 381.
[9] K. Tiefenthaler, *Adv. Biosensors* **1992**, *2*, 261 (a commercial instrument is available from *Artificial Sensing Instruments*, Zürich).
[10] J.J. Ramsden, *J. Molec. Recog.* **1997**, *10*, 109.
[11] J.J. Ramsden, *Experientia* **1993**, *49*, 688.
[12] a) J.J. Ramsden, *Biopolymers* **1993**, *33*, 475; b) L. Guemouri, J. Ogier, J.J. Ramsden, *J. Chem. Phys.* **1998**, *109*, 3265
[13] A. Colotto, K. Lohner, P. Laggner, *J. Appl. Cryst.* **1991**, *24*, 847.
[14] a) J.J. Ramsden, D.J. Roush, D.S. Gill, R. Kurrat, R.C. Willson, *J. Amer. Chem. Soc.* **1995**, *117*, 8511; b) J.J. Ramsden, in 'Biopolymers at Interfaces', Ed. M. Malmsten, Dekker, New York, 1998, Ch. 10.
[15] J.J. Ramsden, G.I. Bachmanova, A.I. Archakov, *Phys. Rev. E.* **1994**, *50*, 5072.
[16] P. Schaaf, J. Talbot, *J. Chem. Phys.* **1989**, *91*, 4401.
[17] J.J. Ramsden, *Biosensors Bioelectronics* **1998**, *13*, 593.
[18] J.J. Ramsden, *Q. Rev. Biophys.* **1994**, *27*, 41.
[19] a) M. Thompson, C.L. Arthur, G.K. Dahliwal, *Anal. Chem.* **1986**, *58*, 1206; b) M Rodahl, F. Höök, B. Kasemo, *Anal. Chem.* **1996**, *68*, 219;
[20] G.L. Hayward, M. Thompson, *J. Appl. Phys.* **1998**, *83*, 2194.
[21] J.J. Ramsden, *Phys. Rev. Lett.* **1993**, *71*, 295.
[22] G. Pólya, *Math. Ann.* **1921**, *83*, 150.
[23] J.J. Ramsden, J. Dreier, *Biochemistry* **1996**, *35*, 3746.
[24] Y. Timsitt, D. Moras, *Q. Rev. Biophys.* **1996**, *29*, 279.